

Analysis of Conductive and Convective Transfers in a Double Salience Switched Reluctance Machine by Analytical Coupling-2D Finite Elements

Badache Souad¹

Abstract: The work presented in this paper concerns the study of the thermal behavior due to copper losses and iron losses of a switched reluctance machine with double salience (SRM6/4) by analytical coupling – 2D finite elements. Calculation by analytical methods of the conduction coefficients in the radial and axial direction as well as the convection coefficients in the air gap of this machine are presented. The values of these found coefficients are used to solve the transient thermal problem for this device using the ADEMEF2D software. The obtained results show a very large increase in temperature at the winding. Heat conduction in both radial and axial directions has a very large effect on the temperature value in all regions of the SRM6/4.

Keywords: Switched reluctance machine, Thermal analysis, Finite elements.

1 Introduction

Any thermal study of electrical machines aims to evaluate the distribution of temperature to improve materials, geometry, or cooling system in order to predict certain operating that can reduce their life. Like any actuator the switched reluctance machine, during its operation, heats up and the essential origin of its heating is due to Joule losses, iron losses, mechanical losses and other physical phenomena impossible to evaluate. To quantify these phenomena, three modes of heat transfer are used: conduction, convection and radiation. For a complete thermal analysis, it is imperative to calculate the different heat exchange coefficients (conduction, convection and radiation) in the different parts of the machine. It is in this concept that several studies have been carried out using the equivalent thermal circuit method [1 – 4]. Although old, this method is still used in thermal calculations of electrical machines. Two and three dimensional finite elements method is also used [5 – 7]. It is a booming digital method due to the planned couplings. Only, in all these studies, certain data are not taken into account. For heat sources, iron losses are

¹University of Science and Technology Mohamed Boudiaf, B. P 1505-Oran, El Mnaouer 31000, Algéria;
Email: badachesouad@yahoo.fr

generally neglected. Furthermore, the heat transfer coefficients by conduction in both axial and radial directions as well as by convection for a notched air gap (case of SRM6/4) have not been sufficiently addressed.

In this work, we will use the 2D finite elements method (MEF2D) to analyze the different heat transfers in SRM6/4. Our main contribution is to provide elements of response to some unsolved problems in this area, particularly for the calculation of the heat transfer coefficients where coupling between analytical and numerical calculations by MEF will be carried out. Since thermal radiation is a mode of transfer with little influence in electrical machines [8], the analysis will only concern the phenomena of conduction and convection. We will first present the equations necessary to model heat transfers in electrical machines, then we will discuss their use for thermal modeling of SRM6/4 by the MEF2D and we will present our simulation results.

2 Heat Transfers in Electrical Machines

2.1 Conductive transfers

Conduction is defined as the mode of heat transmission caused by the difference in temperature between two regions of a solid, liquid or gaseous medium, or between two media in physical contact [9]. In the case of electrical machines, the conductivity of materials is generally well known, except the case of that of magnetic sheets. Indeed, a stack of sheets constitutes the stator and the rotor. The thermal conductivity in the orthoradial direction is known and corresponds to that of the steel constituting the sheets. The situation is different for the axial direction. The sheets are thin and impregnated with varnish, which creates a thermal resistance difficult to evaluate. The axial thermal conductivity of the sheet package will then be lower than that in the radial direction [10]. This is the opposite of the case of windings, in which the axial thermal conductivity is similar to that of pure copper ($\lambda = 400 \text{ W/m/K}$) while the radial thermal conductivity is significantly lower ($\lambda < 1 \text{ W/m/K}$). As a result, because of this difference in thermal conductivities between the two directions, the maximum temperature is often found at the coil heads [11]. The expression of the axial equivalent thermal conductivity is given as below [8, 12]:

$$\lambda_{axiale} = \frac{\lambda_{cuivre} S_{cuivre} + \lambda_{email} S_{email} + \lambda_{vernis} S_{vernis} + \lambda_{air} S_{air}}{S_{cuivre} + S_{email} + S_{vernis} + S_{air}}, \quad (1)$$

where λ_i and S_i are respectively the thermal conductivity and the surface in the radial direction of copper, enamel, varnish and air in the notch.

The thermal conductivity of the copper is at least 400 times higher than of the enamel, varnish and air; the axial thermal conductivity therefore depends almost only on that of the copper and the filling ratio. Several researchers have

tried to find generic analytical expressions for the equivalent radial heat conductivity.

Among them, the authors in reference [13] found a correlation between the equivalent radial thermal conductivity (λ_{radial}), the notch surface (S_{notch}), the active length (L_a) and the filling coefficient (K_b) as below:

$$\lambda_{axiale} = 0.2425[(1 - K_b)S_{notch}L_a]^{-0.04269}. \quad (2)$$

For low power electrical machines, the proposed method allows us to obtain satisfactory results. For high-power electrical machines, the presence of fluid circulation in the core of the conductors prohibits this globalization in the representation of the winding [14].

The shaft and the housing are often massive, the radial and axial thermal conductivity are identical.

2.2 Convective transfers

Convection is the mode of transmission that involves the displacement of a liquid or gaseous fluid. This mode of transfer is found in the exchange between a wall and a fluid. In the case of forced convection, the movement of the fluid is due to the action of a pump or a fan. In natural convection (free), the movement of the fluid is created by a difference of densities, themselves due to differences of existing temperatures in the fluid [15].

The convective heat transfer in electrical machines is produced between the solid surfaces of the machine and the fluid medium, in or around the machine: between the outer surface of the rotor and the air gap, between the inner surface of the stator and the gap, between the outer surface of the stator and the environment and between the coil heads and the surrounding fluid. The global phenomenon of convection can be expressed by the following relation:

$$\varphi = hS(T - T_e), \quad (3)$$

where h is heat transfer coefficient [$\text{Wm}^{-2}\text{K}^{-1}$], S is area of the cross section through the heat flux [m^2], T_e is surrounding temperature (fluid) [K] and T is body surface temperature [K].

The relation giving the coefficient of exchange by convection is expressed by:

$$h = \lambda N_u / L, \quad (4)$$

where N_u is the number of Nusselt [without dimensions], λ is the thermal conductivity of the fluid [$\text{Wm}^{-1}\text{K}^{-1}$] and L is characteristic length of the exchange surface [m].

The value of the Nusselt number depends on the type of convection (natural, forced). In a general way, the relations giving the value of Nusselt depend on the nature of the convection. In the case of a natural convection N_u

depends on the number of Prandtl P_r and the number of Grashof G_r . The general forms of these coefficients are as follows:

$$N_u = a(G_r P_r)^b, \quad (5)$$

$$P_r = \frac{C_p \mu}{\lambda}, \quad (6)$$

$$G_r = \frac{\beta g \Delta T \rho^2 L^3}{\mu^2}, \quad (7)$$

where C_p is the heat capacity of the fluid [$\text{Jkg}^{-1}\text{K}^{-1}$], μ is the dynamic viscosity of the fluid [$\text{kgs}^{-1}\text{m}^{-1}$], β is the coefficient of cubic dilation of the fluid [K^{-1}], g is the gravitational force [ms^{-2}], ΔT is the temperature difference between the surface and the fluid [K] and L is the characteristic length of the exchange surface [m].

On the other hand, and in the case of a forced convection, N_u depends on the Reynolds number R_e . The general forms of these coefficients are as follows:

$$N_u = a(R_e)^b (P_r)^c, \quad (8)$$

$$R_e = \frac{\rho v D_h}{\mu}, \quad (9)$$

where ρ is the density of the fluid [kgm^{-3}], v is the fluid velocity [ms^{-1}], a , b and c are the experimentally determined constants.

In the case of a forced convection, the Reynolds number makes it possible to determine if the flow is laminar or turbulent. For a simple annular geometry, it is often preferred to use the Taylor number instead of the Reynolds number. It is therefore this modeling that is most often used for the study of the heat transfers in the air gap of electrical machines [16].

2.2.1 Convective transfers in the air gap

The air gap is the seat of a rotation flow, there are several correlations that allow to define the number of Nusselt according to the configuration of the gap. The formulation of this number can be different according to the authors and often involves the square of the speed of rotation. In general, the Taylor number is expressed as follows [16]:

$$T_a = \frac{\omega^2 r_m e^3}{v^2 F_g}, \quad (10)$$

$$r_m = \frac{e}{\ln(r_e/r_i)}, \quad (11)$$

where e is the width of the gap [m], r_m is the average log radius [m], ν is the kinematic viscosity [m^2s^{-1}], ω is the angular velocity of the rotor [rads^{-1}], r_e and r_i are respectively the inner radius of the stator and outer radius of the rotor.

F_g is a geometric factor that allows to take into account the shape ratio of the annular space. Its value is very close to unity for a narrow air gap, and is defined by the expression:

$$F_g = \left(\frac{\pi}{1697P} \right) \left(\frac{r_i + r_e}{2r_i} \right), \quad (12)$$

where

$$P = 0.0571 \left(1 - 0.652 \frac{e}{r_i} \right) + 0.00056 \left(1 - 0.652 \frac{e}{r_i} \right)^{-1}. \quad (13)$$

The Nusselt number used to calculate the convection coefficient depends on the Taylor number. The nature of the flow is laminar and the rotational speed does not influence the value of the exchange coefficient up to a critical value of the Taylor number. Beyond this value, the flow switches from laminar to turbulent flow and the value of Nusselt depends on the speed of rotation.

2.2.1.1 Smooth air gap

In the case of a smooth air gap, the critical value of the Taylor number is close to 1700 and the correlations, making it possible to calculate the Nusselt number in this case, are [16]:

$$\begin{aligned} T_a < 1700, \quad N_u &= h2e/\lambda = 2, \\ 1700 < T_a < 12000, \quad N_u &= 0.128T_a^{0.367}, \\ 12000 < T_a < 4 \cdot 10^6, \quad N_u &= 0.409T_a^{0.241}. \end{aligned} \quad (14)$$

2.2.1.2 Non-uniform air gap

Some authors [17] have proposed correlations for obtaining the Nusselt number. In the presence of a non-uniform air gap, the critical value of the Taylor number becomes larger than in the case of a smooth air gap. The transition to vortex flow is then delayed. The critical value of the Taylor number is in this case about 6000:

$$\begin{aligned} T_a < 6000, \quad N_u &= h2e/\lambda = 2, \\ 6000 < T_a < 1.4 \cdot 10^6, \quad N_u &= 0.364T_a^{0.3}, \\ 1.4 \cdot 10^6 < T_a < 2 \cdot 10^7, \quad N_u &= 0.058T_a^{0.4}. \end{aligned} \quad (15)$$

3 Presentation of the Study Machine

We chose to do the thermal study in the case of a switched reluctance machine with six poles at the stator and four poles at the rotor. This actuator must operate according to a specification determined for use in an electric vehicle [18]. The speed being 2500 rpm, the torque to be provided is 103 Nm and the power is 27 kW. The voltage of the power source is 120 V. The phase-calculated Joule losses are 540W. The estimated iron losses are around 862W. In Fig.1 we show the 2D geometry of the study SRM 6/4 and in **Table 1** we give in mm, its main dimensions.

4 Results

In electrical machines, heat conduction takes place in the radial direction and the axial direction. The study is two-dimensional. We made a radial section of the study machine (Fig. 1). We assume that the heat transfers are done radially. The machine is of low power, there is no circulation of fluid at the heart of the conductors, so we applied (2) to calculate the equivalent radial thermal conductivity of the stator notches. The value found is 0.3304W/m°C. This low value is due to the use of insulation in the conductors. For the magnetic circuit, the value of the radial thermal conductivity is that of the used iron which is in our case the Fe-Si.

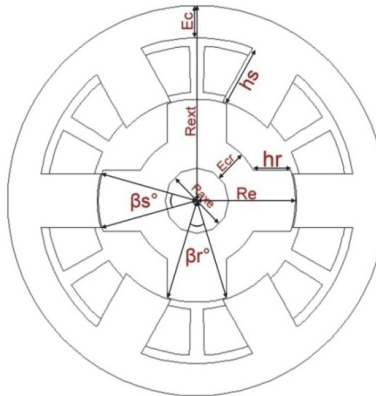


Fig. 1 - Geometry of the SRM6 / 4.

The SRM 6/4 has a non-uniform air gap. The maximum operating speed of the machine is 2500 rpm. Without fan mounted on the rotor, we have no axial fluid flowing in the air gap. We calculated the Taylor number with the expression (10). We obtained a Taylor number maximum value of 4151, which is lower than the Taylor critical number. Thus, we can consider that the presence of the grooves in the stator and in the rotor has no influence on the

convection in the air gap, hence $N_u = 2$ and the value of the convection coefficient in the air gap calculated by (15) is $32.75\text{W}^{\circ}\text{Cm}^2$. This coefficient can only be applied to regions 6, 7, 8, 9, 10 and 11; for the other regions, (4) and (5) are used to calculate the natural convection coefficient. The results are given in Fig. 2 and **Table 2**.

Table 1
Dimensions of the SRM6/4.

| | | | |
|-----------|---------|-----------|----------------|
| R_{ext} | 125 mm | h_s | 38.5 mm |
| R_e | 65 mm | β_s | 30° |
| R_{axe} | 21 mm | β_r | 35.1° |
| L_a | 150 mm | h_r | 23 mm |
| E_c | 20.5 mm | E_{cr} | 21 mm |

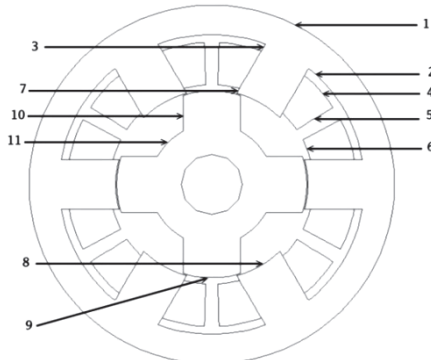


Fig. 2 – Different regions of convective transfers.

Table 2
Convection coefficients h for each region.

| Regions | Coefficient h [$\text{W}^{\circ}\text{Cm}^2$] |
|------------|--|
| Region(1) | 5.86 |
| Region(2) | 8.86 |
| Region(3) | 15.60 |
| Region(4) | 11.18 |
| Region(5) | 11.21 |
| Region(6) | 32.75 |
| Region(7) | 32.75 |
| Region(8) | 32.75 |
| Region(9) | 32.75 |
| Region(10) | 32.75 |
| Region(11) | 32.75 |

We have studied the distribution of temperature and its evolution as a function of time in the different parts of the machine using 2D ADEMEF2D finite element software. The values of thermal conductivities, heat capacities and densities of materials for each region are given in **Table 3**. The applied boundary conditions are of the convection type resulting from the preceding results with an ambient temperature of 25°C. We only excited a single coil.

Table 3
Properties of materials.

| | Thermal Conductivity [W/°Cm] | Heat capacity [J/kg °C] | Density [kg/m ³] |
|--------|---------------------------------|----------------------------|---------------------------------|
| Air | 2.62e ⁻² | 1006 | 1.177 |
| Fe-Si | 84 | 460 | 7600 |
| Copper | 0.33-395 | 385 | 8918 |

In the first case we used a copper heat conductivity of 0.33 W/°Cm. The results show a very large increase in temperature at the excited coil and its vicinity reaches a temperature of around 190°C after one hour of operation. Fig. 3 shows this temperature distribution. We found that there is a very large temperature difference between the coil and the other regions. This difference is around 90°C.

In the second case we used a copper thermal conductivity of 395W/°C, without taking into consideration the direction (axial or radial). The results show an increase in temperature at the excited coil and its vicinity reaches a temperature of 90°C after one hour of operation.

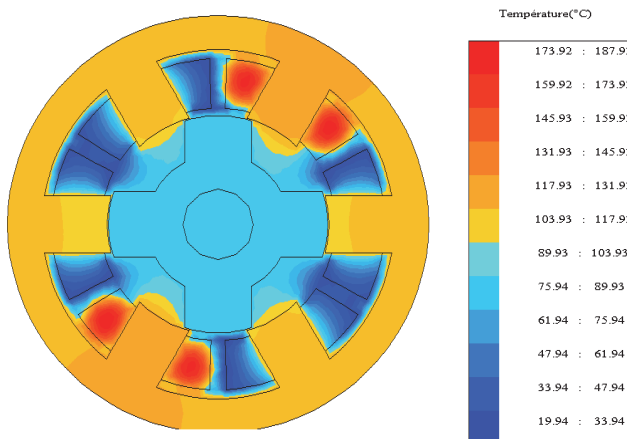


Fig. 3 –Distribution of the temperature in color gradients after 1h of walking, case (1).

Fig. 4 shows this temperature distribution. We have noticed that the heat has spread rapidly to other regions and the difference in temperature between the coil and its vicinity is not important, about 20°C only. Fig. 5 shows the evolution of temperature as a function of time. We took a point in some regions (stator, rotor and coil) for both cases and plotted the temperature variation over time for these regions. We noticed that the temperature increase is very rapid during the first few minutes and then begins to be slow until it becomes constant.

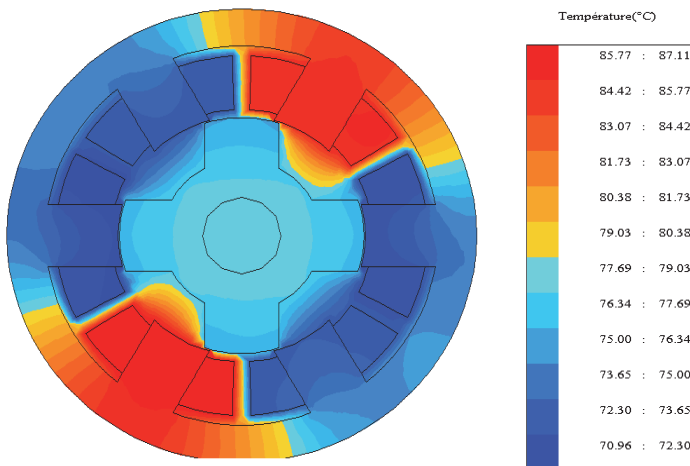


Fig. 4 – Distribution of the temperature in color gradients after 1h of walking, case (2).

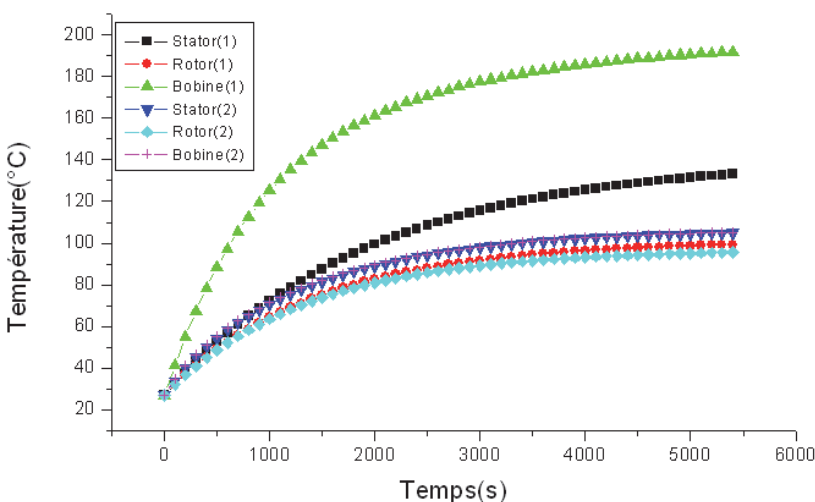


Fig. 5 – Evolution of the temperature as a function of time.

5 Conclusion

In this paper, we presented a modeling of thermal phenomena in a switched reluctance machine. This modeling took into account the heat transfer by conduction and by convection using the transient regime and based only on iron losses and Joule losses as heat sources. To solve the different equations of this modelization, we used the finite element method in two dimensions. We considered an SRM6/4 machine in which the air gap is not uniform. This has confronted us with several difficulties in particular for the conduction coefficients whose calculation in the radial direction is different from the axial one, as well as for the convective boundary conditions where several parameters must be highlighted. The study showed that the geometry of the SRM6/4 presents particular difficulties and its heterogeneous structure composed of several materials complicates the determination of the temperature distribution which mainly depends on heat transfers in different directions. Indeed, only a 3D study can give an account of the real thermal behavior of this machine. The effect of conduction in the axial direction and the existence of a thermal effect due to radiation could be taken into account in future studies.

6 References

- [1] J. Faiz, A. Dadgari: Heat Distribution and Thermal Calculations for Switched Reluctance Motors, Proceedings of the 5th International Conference on Electrical Machines and Drives, London, UK, September 1991, pp. 305 – 310.
- [2] A. Matveev: Development of Methods, Algorithms and Software for Optimal Design of Switched Reluctance Drives, Ph. D. Dissertation, Eindhoven University of Technology, Eindhoven, Nederlanden, 2006.
- [3] H. Rouhani, J. Faiz, C. Lucas: Lumped Thermal Model for Switched Reluctance Motor Applied to Mechanical Design Optimization, Mathematical and Computer Modelling, Vol. 45, No. 5-6, March 2007, pp. 625 – 638.
- [4] S. Shoujun, L. Weigu, D. Peitsch, U. Schaefer: Detailed Design of a High Speed Switched Reluctance Starter/Generator for More/All Electric Aircraft, Chinese Journal of Aeronautics, Vol. 23, No. 2, April 2010, pp. 216 – 226.
- [5] K. N. Srinivas, R. Arumugam: Thermal Characterization Through Finite Element Analysis of the Switched Reluctance Motor, Proceedings of the IEEE Region 10 International Conference on Electrical and Electronic Technology (TENCON), Singapore, Singapore, August 2001, pp. 819 – 823.
- [6] S. Inamura, T. Sakai, K. Sawa: A Temperature Rise Analysis of Switched Reluctance Motor Due to the Core and Copper Loss by FEM, IEEE Transactions on Magnetics, Vol. 39, No. 3, May 2003, pp. 1554 – 1557.
- [7] K. N. Srinivas, R. Arumugam: Analysis and Characterization of Switched Reluctance Motors: Part II. Flow, Thermal and Vibration Analyses, IEEE Transactions on Magnetics, Vol. 41, No. 4, April 2005, pp. 1321 – 1332.
- [8] Y. Bertin: Cooling of Rotating Electrical Machines, Techniques de L'Ingénieur, Conversion de l'énergie électrique, D3460, May 1999, pp. 1 – 20. (In French).

- [9] M. A. Sefouane: Distribution of the Temperature Field in Cylindrical Metal Parts Heated by Magnetic Induction by a Numerical Method (MEF), Final thesis for obtaining the engineering degree, Chlef University Center, Algeria, Algeria, 1999. (In French).
- [10] A. Fasquelle: Contribution to Multi-Physics Modeling: Electro-Vibro-Acoustic and Aerothermic Traction Machines, Ph. D. Dissertation, Doctoral school SPI 072, Lille, France, 2007. (In French).
- [11] J. Nerg, M. Rilla, J. Pyrhonen: Thermal Analysis of Radial-Flux Electrical Machines with a High Power Density, IEEE Transactions on Industrial Electronics, Vol. 55, No. 10, October 2008, pp. 3543 – 3554.
- [12] R. Glises, R. Bernard, D. Chamagne, J. M. Kauffmann: Equivalent Thermal Conductivities for Twisted Flat Windings, Journal de Physique III, Vol. 6, No. 10, October 1996, pp. 1389 – 1401.
- [13] A. Boglietti, A. Cavagnino, D. Staton: Determination of Critical Parameters in Electrical Machine Thermal Models, IEEE Transactions on Industry Applications, Vol. 44, No. 4, July 2008, pp. 1150 – 1159.
- [14] G.- J. Li: Contribution to the Design of Passive Rotor Electrical Machines for Critical Applications: Electromagnetic and Thermal Modeling on Cyclic Operation, Study of Degraded Mode Operation, Ph. D. Dissertation, ENS Paris-Saclay, Cachan, France, 2011. (In French).
- [15] A. B. de Vriendt: The Transmission of Heat, Gaëtan Morin, Vol. 1, Paris, 1982. (In French).
- [16] M. L. Idoughi: Extraction of Simplified Thermal Models of Electrical Machines from a Calculation of the Temperature Field, Ph. D. Dissertation, Paris-Sud University, Paris, France, 2012.
- [17] M. Bouafia, Y. Bertin, J. B. Saulnier, P. Robert: Experimental Analysis of Heat Transfer in a Narrow and Grooved Annular Gap with Rotating Inner Cylinder, International Journal of Heat and Mass Transfer, Vol. 41, No. 10, May 1998, pp. 1279 – 1291. (In French).
- [18] E. Hoang: Study, Modeling and Measurement of Magnetic Losses in Double-Slip Variable Reluctance Motors, Ph. D. Dissertation, ENS Paris-Saclay, Cachan, France, 1995. (In French).